Published in Applied Physics Letters 76, 2337-2339, 2000
which should be used for any reference to this work

Realization of a complex-coupled InGaN/GaN-based optically pumped multiple-quantum-well distributed-feedback laser

Daniel Hofstetter,[a] Linda T. Romano,[b] Thomas L. Paoli, David P. Bour, and Michael Kneissl
Xerox Palo Alto Research Center, 3333 Coyote Hill Road, Palo Alto, California 94304

We demonstrate an optically pumped complex-coupled InGaN/GaN-based multiple-quantum-well distributed-feedback laser in the violet/blue spectral region. The third-order grating providing feedback was defined holographically and dry etched through a portion of the active region by chemically assisted ion-beam etching. Epitaxial overgrowth of the GaN waveguide completed the device structure without introducing dislocations, as shown by transmission electron microscopy. The laser emitted light at 392.7 nm with high side-mode suppression and a narrow linewidth of 1.5 Å. In contrast to Fabry–Pérot lasers fabricated from the same piece of material, only a very minor change in emission wavelength was observed when operating the device at higher pump intensities.

Short-wavelength semiconductor lasers are very attractive light sources for both data storage and scanning applications. During the last few years, both pulsed and continuous-wave operation of InGaN/GaN-based blue lasers have been demonstrated at room temperature.[1,2] Most research groups have typically used sapphire substrates for GaN growth. However, the misorientation between the sapphire and the GaN cleavage planes does not readily permit cleaving of the facets. Dry-etched mirrors with high-reflective coatings appear to work satisfactorily in this material system,[3] but there is still a certain need to improve the cavity properties of nitride lasers, especially as far as mode selection is concerned. The use of distributed feedback (DFB) has already been explored somewhat for the purpose of improved mode and wavelength stability. Consequently, optically pumped[4,5] and electrically injected DFB lasers[6] in the InGaN/GaN material system have been reported recently. These devices were based on index coupling between the forward and backward propagating modes, which usually leads to additional loss through scattering at the corrugated interface between the waveguide and the cladding layer. Also, index coupling tends to be weak for higher-order gratings with nonideal tooth shape. Hence, we describe in this letter the fabrication of a nitride-based multi-quantum-well (MQW) DFB laser with a complex-coupled (i.e., index- plus gain-coupled) third-order grating, which enables increased coupling strength and potentially lower threshold intensity.

Fabrication of this device began with growth of a 4-μm-thick GaN:Si layer on *c*-face sapphire. On top of this layer, we grew a 500-nm-thick $Al_{0.08}Ga_{0.92}N$:Si lower cladding layer, a 100-nm-thick GaN lower waveguiding layer, and a 40-nm-thick active region with five $In_{0.1}Ga_{0.9}N$ quantum wells (QWs) and GaN barriers. A 10-nm-thick $Al_{0.2}Ga_{0.8}N$:Mg overlayer and a 20-nm-thick portion of the GaN upper waveguiding layer completed this first growth step. The third-order grating with a period of 240 nm was then defined by holographic exposure by using two-beam interference with a 325 nm UV HeCd laser. Transfer into the semiconductor was achieved by dry etching in a chemically assisted ion-beam etching (CAIBE) system.[7] We then overgrew the etched surface with a (second) 10-nm-thick $Al_{0.2}Ga_{0.8}N$:Mg overlayer and a nominally 150-nm-thick GaN:Mg upper waveguide layer. This configuration allowed optical pumping through the surface. After optical pumping studies, we overgrew both structures with a 300 nm $Al_{0.08}Ga_{0.92}N$:Mg upper clad layer and a GaN:Mg contact layer.

Using the holographic process described above usually resulted in an oval-shaped grating area, which measured 6×10 mm^2 in size. Precise control of photoresist thickness and etch rate was required in order to accurately define a grating that extended into the active region. Small variations in photoresist thickness defining the etch mask and etch rate could easily result in an insufficient corrugation amplitude or overetching of the grating. Since the photoresist thickness is difficult to control, we usually observed, even within a small area, a gradually changing etch-depth and line-to-space ratio.

In the following, two different samples (A and B) were investigated. In sample A, a thick photoresist mask was used to etch a grating with a depth of 65 nm. As a result of this, we obtained an active region with, typically, 2–3 etched QWs. On the other hand, sample B had a thinner photoresist layer, which resulted in a shallower (40-nm-deep) grating that was slightly overetched. The corrugation amplitude with an overetched depth of 40 nm was sufficient to punch through most of the active region and form wire-like sections of active material. However, the overetching removed the $Al_{0.2}Ga_{0.8}N$:Mg overlayer and the top QW in this sample. Figures 1(a) and 1(b) show schematic cross sections through both devices after completion of the first regrowth.

For an assessment of the material's quality after ion-beam etching into the active region, we carried out photoluminescence measurements (PL) of sample A. A 325 nm

[a]Present address: University of Neuchâtel, 1 A.-L. Breguet, CH-2000 Neuchâtel, Switzerland; electronic mail: hofstetter@iph.unine.ch
[b]Author to whom correspondence should be addressed; electronic mail: romano@parc.xerox.com

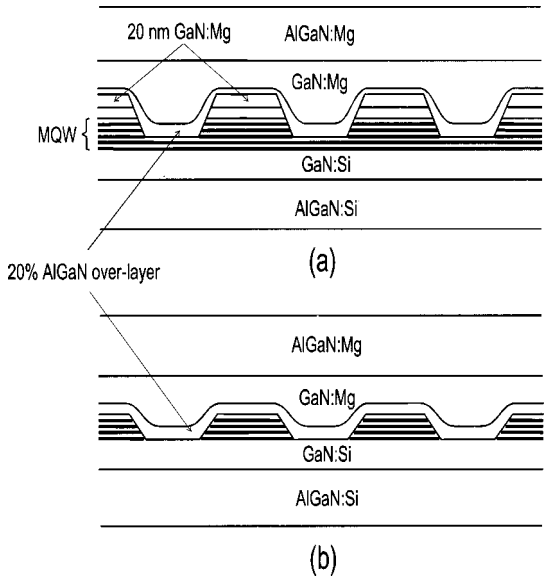

FIG. 1. (a) Schematic cross section through sample A after regrowth. (b) Schematic cross section through sample B after regrowth. Layers labeled ''AlGaN:Si/Mg'' are lower/upper cladding layers, those labeled ''GaN:Si/Mg'' are lower/upper waveguide layers.

HeCd laser was used as the excitation light source and the measurements were carried out at room temperature. The PL spectra from the as-grown sample, a region of material from the edge of the DFB grating, and the region of material from the (most heavily etched) center of the grating region are shown in Fig. 2. They clearly reveal a decreasing intensity of the blue band-edge emission at 400 nm and an increasing amount of yellow, defect-related luminescence centered at 500 nm. The decreasing blue emission is mainly due to the reduced amount of active material and defect states induced by the CAIBE. The yellow luminescence stays constant for both areas exposed to the etching process and does not seem to depend strongly on the amount of etched active material, suggesting it arises at or near the etched interface.

Cross-section transmission electron microscopy (TEM) samples were prepared in the usual manner by polishing and ion-beam thinning to electron transparency with an Ar beam at low voltage (~3 kV) and with the sample mounted on a

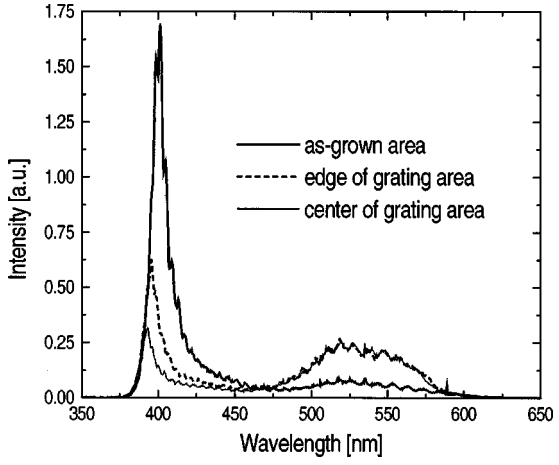

FIG. 2. Room-temperature photoluminescence spectra at three different locations on the sample going from an unetched corner towards the center of the grating region.

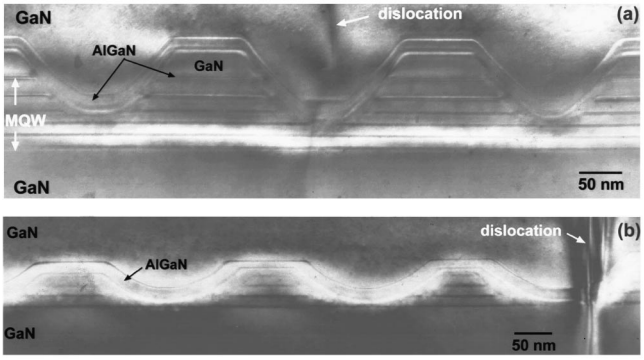

FIG. 3. (a) Cross-sectional TEM picture of the active region of sample A after regrowth. (b) Cross-sectional TEM picture of the active region of sample B after regrowth.

liquid-nitrogen cold stage in order to minimize ion damage. The samples were oriented for TEM observation to be parallel to the grating normal which was either along the $\{10\underline{1}0\}$ or $\{11\underline{2}0\}$ crystallographic direction of the GaN. Figure 3(a) shows a TEM cross-sectional image of the active region of sample A that showed lasing. The image is taken near the $\{10\underline{1}0\}$ zone axis with diffraction vector $\mathbf{g}=0002$ to highlight the atomic number contrast from the different layers. Threading dislocations that initiated near the sapphire substrate are observed to extend through the grating and continue to the film surface. However, in combination with other images taken with **g** parallel to the interface, no structural defects were found at the grating interface. This is similar to our earlier observations of index-coupled DFB lasers, although the grating in that case consisted of an AlGaN layer over a GaN grating,[8] instead of an AlGaN layer over an InGaN grating as shown here. We note, however, that the consequences of a threading dislocation may be more detrimental in the current structure, because we are effectively reducing the amount of active material required for lasing. Since the TEM image shows that 2–3 out of 5 QWs were etched, this sample illustrates a complex-coupled DFB laser. Figure 3(b) is a cross-sectional TEM image of sample B showing that 3–4 QWs were etched to form the grating. Similar to sample A, no additional dislocations are introduced at the grating interface after regrowth. From the TEM image of sample B, we observe that approximately 30% of the active material remains after etching. This sample is also a complex-coupled DFB device, but with a larger component due to gain coupling. For both samples, we estimated similar amounts of complex coupling ($\kappa=5$–10 cm^{-1} each) with a slightly smaller number for the gain-coupling coefficient in sample A compared to sample B.

Optical pumping was carried out as described earlier using a pulsed 337 nm N_2 laser ($r_{\text{pulse}}=10$ Hz, $P_{\text{peak}}=250$ kW) whose stripe-shaped beam was attenuated by an appropriate number of glass slides. The output of the InGaN/GaN laser was fed into either a high-resolution spectrometer (for linewidth measurements) or a low-resolution grating spectrometer (for output intensity versus current curves). The pieces on which we performed these experiments were approximately 10×10 mm^2 in size, and all four facets were fabricated by scribing from the back and subsequent cleaving. Although this method resulted in a poor Fabry–Pérot (FP)

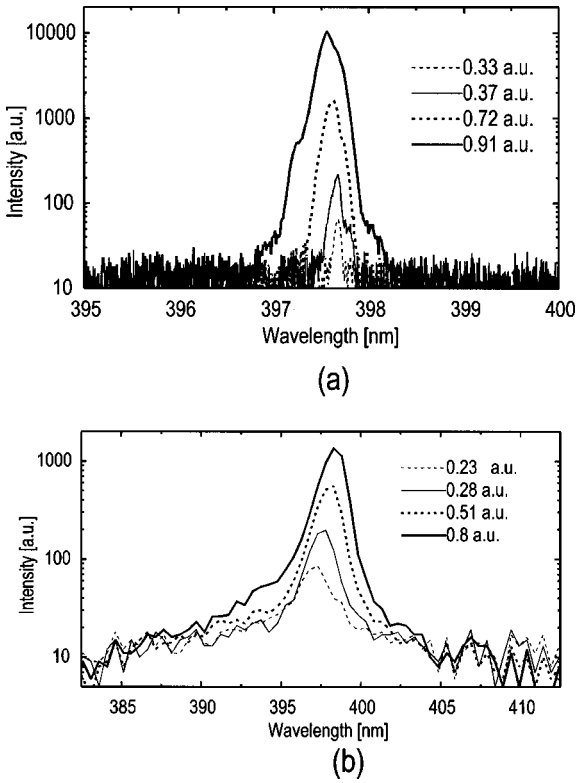

FIG. 4. High-resolution emission spectrum of an optically pumped complex-coupled DFB laser at various pump intensities. (b) Low-resolution emission spectrum of an optically pumped FP laser at various pump intensities.

cavity and, in addition, the N_2 laser beam was pumping only 30%–40% of the cavity length, FP-type laser emission could be observed as well as DFB laser emission. The orientation of the grating lines relative to the pump beam determined which emission was dominant.

Typical emission spectra of DFB-type lasing are shown in Fig. 4(a). The emission peak stays at 392.7 nm from threshold up to 0.9 a.u. pump intensity. It shifts somewhat towards shorter wavelengths at higher pump intensities. The reason for this wavelength shift is a slight reduction of the effective refractive index at high carrier density that overwhelms the relatively small index increase due to the device heating. The linewidth change from 1.5 Å right above threshold to 3.0 Å at 0.8 a.u. is likely due to lateral multimode operation and chirping at high pump intensities. In Fig. 4(b), we show a series of low-resolution emission spectra for the FP emission of sample A. The FP emission peaks at 397 nm with a typical linewidth of around 25 Å. In contrast to the DFB laser spectra, we see for the FP laser a pronounced redshift of the lasing peak as the pumping level is increased. While the DFB lasing wavelength is locked to the Bragg resonance wavelength, the emission of the FP follows the gain maximum, which, due to heating-induced band-gap shrinkage, shifts rapidly towards longer wavelengths.

For sample B, lasing threshold could not be reached. This is attributed to the small amount of active material left after etching, possible CAIBE damage, and finally, a relatively large mismatch between the Bragg resonance wavelength and the gain peak. Very intense optical pumping was necessary to reach threshold gain in sample A, especially in the areas where the largest fraction of active material was removed. This intense optical pumping caused band filling, which shifted the gain peak towards even shorter wavelengths (388 nm) and further away from the Bragg resonance wavelength (392.7 nm). From intensity measurements taken below threshold, we estimated the gain of sample A peaked at 397 nm with a full width at half maximum of 11 nm, indicating that both FP and DFB lasing wavelengths were within the gain peak of the material. Measurements of the pump versus output intensity characteristics were carried out at room temperature. They showed comparable intensity thresholds of around 0.35 a.u. for the DFB and 0.25 a.u. for the FP laser, which corresponds roughly to 3.5 and 2.5 MW/cm^2, respectively. For sample A, we quantitatively characterized the far-field patterns of both the FP and the DFB emission. Due to the absence of an AlGaN upper cladding layer, the result of these measurements was similar to our previous reports[5] on optically pumped InGaN/GaN lasers. In the vertical direction, the far field revealed two main emission lobes at angles of around $\pm 34.5°$ to the horizontal and a number of weaker intensity maxima in between.

In conclusion, we have demonstrated a short-wavelength optically pumped complex-coupled InGaN/GaN-based MQW DFB laser. The threshold intensity was on the order of 3.5 MW/cm^2 and somewhat higher than in FP-type lasers. The emission of the DFB laser was at a wavelength of 392.7 nm and was as narrow as 1.5 Å compared to 397 nm and 25 Å for the FP emission. The primary emission peak did not markedly change its wavelengths over a range of pump intensities, which indicates strong coupling to the grating resonance peak.

The authors would like to thank Fred Endicott and Greg Anderson for help in setting up the experiment; Gary Evans from Southern Methodist University, Dallas, TX, for valuable discussions; and Noble M. Johnson and Ross Bringans for helpful support. This work was supported by the Defense Advanced Research Projects Agency (DARPA Contract No. MDA 972-96-3-0014), and the Swiss National Science Foundation.

[1] S. Nakamura, M. Senoh, S. Nagahama, N. Iwasa, T. Yamada, T. Matsushita, Y. Sugimoto, and H. Kiyoku, Jpn. J. Appl. Phys., Part 2 **35**, L74 (1996).
[2] S. Nakamura, M. Senoh, S. Nagahama, N. Iwasa, T. Yamada, T. Matsushita, Y. Sugimoto, and H. Kiyoku, Appl. Phys. Lett. **72**, 211 (1998).
[3] M. Kneissl, D. Hofstetter, D. P. Bour, R. Donaldson, J. Walker, and N. M. Johnson, J. Cryst. Growth **189/190**, 846 (1998).
[4] R. Hofmann, H. P. Gauggel, U. A. Griesinger, H. Gräbeldinger, F. Adler, P. Ernst, H. Bolay, V. Härle, F. Scholz, H. Schweizer, and M. H. Pilkuhn, Appl. Phys. Lett. **69**, 2068 (1996).
[5] D. Hofstetter, R. L. Thornton, D. P. Bour, M. Kneissl, and C. Dunnrowicz, Appl. Phys. Lett. **73**, 1928 (1998).
[6] D. Hofstetter, L. T. Romano, R. L. Thornton, D. P. Bour, M. Kneissl, and R. M. Donaldson, Appl. Phys. Lett. **73**, 2158 (1998).
[7] I. Adesida, A. T. Ping, C. Youtsey, T. Dow, M. Asif Khan, D. T. Olson, and J. N. Kunzia, Appl. Phys. Lett. **64**, 889 (1994).
[8] L. T. Romano, D. Hofstetter, M. D. McCluskey, and D. P. Bour, Appl. Phys. Lett. **73**, 2706 (1998).